AD-A141 766 REGISTRATION OF A LANDSAT IMAGE TO DTM (DIGITAL TERRAIN MATRIX) - AN ERROR ANALYSIS(U) ARMY ENGINEER TOPOGRAPHIC LABS FORT BELVOIR VA M A CROMBIE ET AL. 1/1

UNCLASSIFIED JAN 84 ETL-0350 F/G 12/1 NL

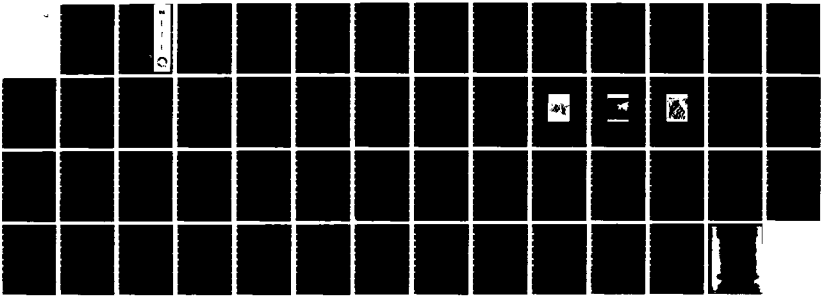

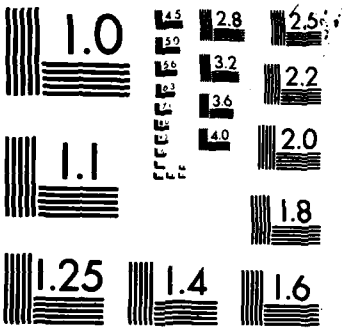

ETL–0350

Registration of a LANDSAT image to a DTM – an error analysis

Michael A. Crombie
James A. Shine
William Moore
Glenn Allton

JANUARY 1984

U.S. ARMY CORPS OF ENGINEERS
ENGINEER TOPOGRAPHIC LABORATORIES
FORT BELVOIR, VIRGINIA 22060

E T L

U.S. ARMY ENGINEER TOPOGRAPHIC LABORATORIES
ETL

UNCLASSIFIED
SECURITY CLASSIFICATION OF THIS PAGE *(When Data Entered)*

REPORT DOCUMENTATION PAGE		READ INSTRUCTIONS BEFORE COMPLETING FORM
1. REPORT NUMBER ETL-0350	2. GOVT ACCESSION NO. AI41766	3. RECIPIENT'S CATALOG NUMBER
4. TITLE *(and Subtitle)* REGISTRATION OF A LANDSAT IMAGE TO A DTM - AN ERROR ANALYSIS		5. TYPE OF REPORT & PERIOD COVERED Research Note 6. PERFORMING ORG. REPORT NUMBER
7. AUTHOR(s) Michael A. Crombie, William Moore James A. Shine, Glenn Allton		8. CONTRACT OR GRANT NUMBER(s)
9. PERFORMING ORGANIZATION NAME AND ADDRESS U.S. Army Engineer Topographic Laboratories Fort Belvoir, Virginia 22060		10. PROGRAM ELEMENT, PROJECT, TASK AREA & WORK UNIT NUMBERS 4A762707A855
11. CONTROLLING OFFICE NAME AND ADDRESS U.S. Army Engineer Topographic Laboratories Fort Belvoir, Virginia 22060		12. REPORT DATE January 1984 13. NUMBER OF PAGES 50
14. MONITORING AGENCY NAME & ADDRESS*(if different from Controlling Office)*		15. SECURITY CLASS. *(of this report)* Unclassified 15a. DECLASSIFICATION/DOWNGRADING SCHEDULE

16. DISTRIBUTION STATEMENT *(of this Report)*

Approved for public release; distribution unlimited.

17. DISTRIBUTION STATEMENT *(of the abstract entered in Block 20, if different from Report)*

18. SUPPLEMENTARY NOTES

19. KEY WORDS *(Continue on reverse side if necessary and identify by block number)*

Digital Image	LANDSAT
DTM	Least Squares
Error Propagation	Pattern Recognition

20. ABSTRACT *(Continue on reverse side if necessary and identify by block number)*

A mathematical model is postulated and tested that will enable a user to relate a digital LANDSAT image to a digital terrain matrix (DTM). The practicality of the procedure is examined and evaluated.

DD FORM 1 JAN 73 1473 EDITION OF 1 NOV 65 IS OBSOLETE

UNCLASSIFIED
SECURITY CLASSIFICATION OF THIS PAGE *(When Data Entered)*

PREFACE

This study was conducted under DA project 4A762707A855, "Topographic Mapping Technology."

The study was done during the summer of 1982 under the supervision of Mr. D. E. Howell, Chief, Information Sciences Division, and Mr. L. A. Gambino, Director, Computer Sciences Laboratory.

A portion of the computer implementation was performed by Cadet Glenn Allton of the Air Force Academy and by Mr. William Moore, a student at Virginia Polytechnic Institute.

COL Edward K. Wintz, CE, was Commander and Director and Mr. Walter E. Boge was Technical Director of the Engineer Topographic Laboratories during the study preparation.

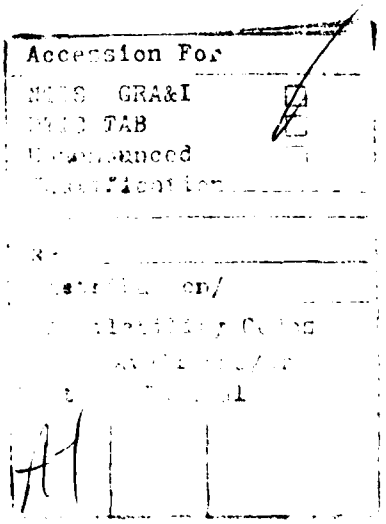

CONTENTS

ILLUSTRATIONS

TABLES

REGISTRATION OF A LANDSAT IMAGE TO A DIGITAL TERRAIN MATRIX—AN ERROR ANALYSIS

INTRODUCTION

One reason for registering a Landsat digital image to a Digital Terrain Matrix (DTM) is to add another dimension to the signature used in scene classification. Ground elevation associated with a pixel can be converted to a terrain slope that, along with orientation with respect to the sun, can be used as an additional component in a pattern recognition exercise. Pixel heights can also be used to restrict the pattern recognition scheme to test over the most likely subset of classes when scene classes can be organized by terrain heights a priori. The purpose of this report is to evaluate the accuracy with which the elevation assignments can be made when the registration process described herein is used.

RELEVANT GEOMETRY

The dynamic Landsat imaging event will be modeled by requiring that the exterior orientation parameters of the camera system be adjusted to fit common data points identified on the DTM and on the Landsat digital image. These parameters include the time-dependent vehicle position and the time-dependent vehicle coordinate frame attitude. The Landsat interior orientation parameters will not be adjusted. These parameters include the detector sizes, the camera focal length, scan angle range, scan angle cycle time, and scan time. The geometry that relates Landsat coordinates (e = line and s = sample) to ground coordinates defined by the DTM is given in detail in appendix A.

Procedure. There are at least two ways to identify common points in the DTM and in the Landsat digital image. In the first case, common points are identified on maps and on Landsat. The common data points will be used to adjust the Landsat geometric model. If the point identification is accurate and if there is negligible bias between the DTM and the map, then the intersection procedure described in appendix A will produce accurate results.

The second procedure relates the DTM and the Landsat digital image directly by viewing both at the same time on separate TV displays. A gray shade relief image is used to transform the DTM into a terrain surface that is recognizable as such (see appendix E). The analyst indicates common points on the two TV displays with cursors. Note that in either pointing, the analyst is in direct communciation with the pertinent data base.

Adjustment Model. At any instant of time, there are six exterior orientation parameters; namely, the three angles that define the attitude matrix of the DTM reference frame with respect to the vehicle frame (M_{GV}) and the three coordinates that locate the vehicle origin in the DTM. The three fundamental angles that define M_{GV} will be modeled as time polynomials. For example, if the fundamental angles are roll (w), pitch (ϕ), and yaw (K), then

$$\begin{pmatrix} w \\ \phi \\ K \end{pmatrix}_t = B\ T_N$$

where

B: 3X(N+1) matrix of attitude constants

$T_N^T = (1, t, t^2, \ldots, t^N)$

Vehicle positions will also be modeled by time polynomials.

$$\begin{pmatrix} X_V \\ Y_V \\ Z_V \end{pmatrix}_t = A\ T_M$$

where

A: 3X(M+1) matrix of position constants

$T_M^T = (1, t, t^2, \ldots, t^M)$

The following discussion describes how second-order time polynomials provide sufficient accuracy for each of the six exterior parameters. In fact, the three attitude parameters can be represented by linear time polynomials with no more than one-half sample spacing error.

The actual Landsat orbit was assumed to follow a Keplerian path, and a 30-second ephemeris in earth-fixed coordinates of such an orbit was developed using the parameter values in table 1.

Table 1. Orbital parameters

T_o = 0.0	:	Time of Perigee Passage
γ_{N_o} = 225^o	:	Longitude of Ascending Node
i = 80.79^o	:	Inclination
w = 135^o	:	Argument of Perigee
e = 0.001019	:	Eccentricity
a = 7285989 meters	:	Semi-Major Axis

Note that γ_{N_o} is measured westward from Greenwich and pertains to time T_o. The inclination is measured counterclockwise at the ascending node. The earth is regarded as a sphere with radius, R = 6,359,550 meters, which means that the Landsat vehicle height is $H \leq (a-R) = 926,439$ meters. A 30-second pass corresponds to a 193.7-kilometer, along-track image, which is larger than the conventional picture.

The vehicle reference frame is nominally oriented so that Z_V is normal to the surface of the earth and so that X_V is tangent to the flight path. The Y_V-axis completes a right-handed system. A set of roll, pitch, and yaw angles was generated for each of the 31 ephemeris positions. These data as well as the position data were fit in turn to linear, quadratic, cubic, and finally to quartic time polynomials. The standard deviations of the residuals were calculated for each of the six exterior orientation values and for each of the four polynominal models. These values represent discrepancies between the Keplerian model and the polynomial models for a 30-second Landsat exposure. The standard deviations are given in table 2. The position discrepancies are expressed in meters and the attitude discrepancies are expressed in seconds of arc.

The total attitude error at Landsat heights (less than 10^6 meters) is less than 0.1 meter per point for the qudratic model, and the total position error is less than 0.7 meter. The corresponding errors for the linear model are 36 meters and 274 meters, respectively. The linear model error for position is large when compared to the Landsat foot print dimension of 79 meters.

Table 2. Model discrepancies

Exterior Orientation

Model	X	Y	Z	ω	φ	κ
Linear	$1.4\text{X}10^{2}$	$1.4\text{X}10^{2}$	$1.9\text{X}10^{2}$	$4.39\text{X}10^{0}$	$2.98\text{X}10^{0}$	$5.17\text{X}10^{0}$
Quadratic	$3.4\text{X}10^{-1}$	$3.8\text{X}10^{-1}$	$5.3\text{X}10^{-1}$	$1.4\text{X}10^{-2}$	$1.3\text{X}10^{-2}$	$8.2\text{X}10^{-3}$
Cubic	$8.4\text{X}10^{-4}$	$6.6\text{X}10^{-4}$	$1.0\text{X}10^{-3}$	$3.1\text{X}10^{-5}$	$3.0\text{X}10^{-5}$	$1.9\text{X}10^{-5}$
Quartic	$4.1\text{X}10^{-4}$	$1.6\text{X}10^{-4}$	$4.1\text{X}10^{-4}$	$9.7\text{X}10^{-6}$	$4.5\text{X}10^{-6}$	$5.3\text{X}10^{-6}$

ERROR ANALYSIS

The 30-second Landsat exposure described above along with the data generator described in appendix C was used to develop 28 sets of exact data. For convenience, the points were defined in a local frame centered at t = 15 seconds. The points are displayed in figure 1 along with the Landsat ground track; the grid spacing in figure 1 is 20 kilometers. Note that the ground tract is from west to east. The reason for this is that the inclination should have been $(\pi-i) = 99^{\circ}.21$, instead of $i = 80^{\circ}.79$. Except for earth rotation, the two situations are exactly symmetric about the pole, which means that using the supplement of the inclination will have no effect on the error analysis of this report.

Least-Squares Adjustment. Five subsets of the 28 ground points were selected to represent five well-distributed control point patterns for adjustment. In addition, four sets of exposure station weights were processed to determine the effect of a priori orbital data on the adjustment. The a priori exposure station standard deviations are given in table 3.

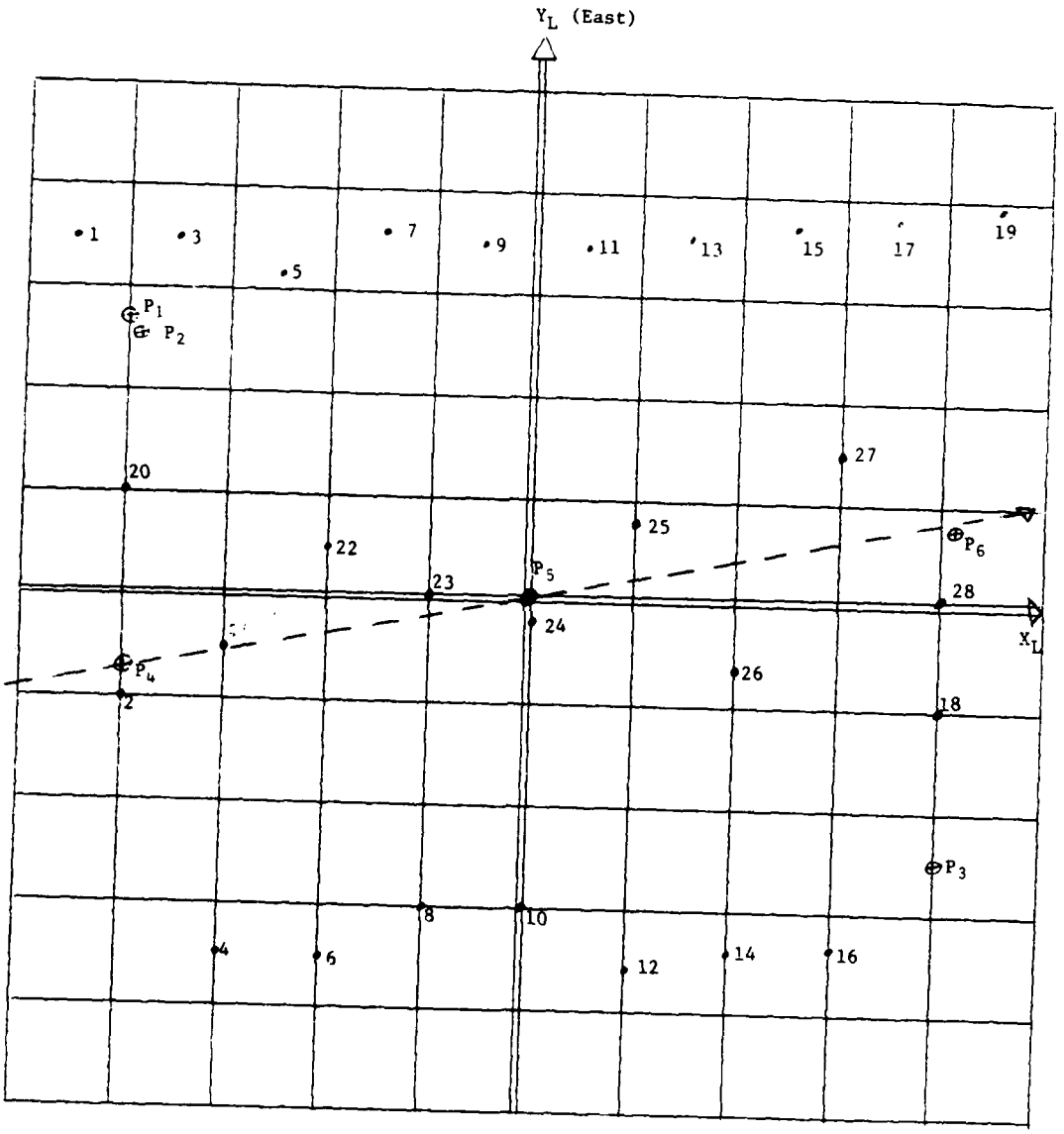

Figure 1. Data points.

Table 3. Landsat ephemeric weights

Weight Model	$\sigma_{c(m)}$	$\sigma_{c(m/sec)}$	$\sigma_{c(m/sec^2)}$
W_1	100	1.0	0.1
W_2	500	2.0	0.2
W_3	1000	5.0	0.5
W_4	2000	10.0	1.0

The five control point patterns are defined in table 4 and are referenced to figure 1.

Table 4. Control point patterns

Control Point Pattern	Number	Points
C_1	28	All 28
C_2	11	#1, #2, #4, #7, #8, #12, #13, #16, #19, #24, #28
C_3	6	#1, #2, #4, #16, #19, #28
C_4	5	#1, #4, #16, #19, #24
C_5	17	#1, #3, #4, #5, #6, #7, #8, #9, #10, #11, #12, #13, #14, #15, #16, #17, #19

The data in tables 3 and 4 were used to develop the several 18 by 18 covariance matrices of the exterior orientation parameter estimates.

Error Propagation. Six points were selected for error propagation. The six points labeled P_1 through P_6 are depicted in figure 1. Points P_4, P_5, and P_6 are equally spaced along the vehicle ground track, while points P_1 and P_3 are diagonally opposite one another. Point P_2 is a close neighbor (5 pixels) of point P_1. Several of the distances are as follows:

$| P_1 - P_2 |$ = 400 meters = 5.1 pixels

$| P_1 - P_3 |$ = 2,000,000 meters = 2531.6 pixels

$| P_4 - P_5 |$ = 81,394.1 meters = 1030.3 pixels

$| P_4 - P_6 |$ = 162,788.2 meters = 2060.6 pixels

The 30-second Landsat exposure and the data generator described in appendix C were used to develop the six sets of Landsat coordinate data. These data and the pertinent (18 x 18) covariance matrix described above were input to the two-point error propagation model described in appendix D. The objective of the exercise was to propagate exterior orientation errors into horizontal errors as functions of the weight model W and the control point pattern C.

The error statement given by equation 4 of appendix D pertains to the geocentric reference system since the exterior data and the control points are expressed in that coordinate frame. In order to express the errors in the local frame, the following transformation must be performed:

$$\sigma_{P_1P_2}\ (\text{Local}) = \begin{pmatrix} A_{GL} & \phi \\ \phi & A_{GL} \end{pmatrix} \sigma_{P_1P_2} \begin{pmatrix} A_{GL}^T & \phi \\ \phi & A_{GL}^T \end{pmatrix}$$

where

A_{GL}: 3 x 3 rotation matrix relating the earth-centered reference frame to the local frame.

ϕ : 3 x 3 zero matrix.

The error propagation results are presented in tables 5 through 8. The first entry is the standard error in the line direction, and the second entry is the standard error in the sample direction; both are expressed in terms of pixels.

Table 5. Standard errors in pixels for W_1

	Points									
Pattern	1	2	3	4	5	6	1-2	1-3	4-5	4-6
C_1	3.4	3.4	4.1	2.9	2.1	3.3	0.01	5.3	3.9	4.0
	0.8	0.8	0.9	0.5	0.6	0.8	0.01	1.0	0.6	0.7
C_2	5.0	5.0	5.9	3.7	3.3	4.8	0.01	7.6	5.4	5.8
	1.0	1.0	1.2	0.6	0.7	0.9	0.01	1.4	0.7	0.9
C_3	12.6	12.5	10.6	6.5	31.8	6.5	0.02	21.2	37.3	10.6
	1.3	1.3	6.1	0.6	1.5	0.9	0.02	5.6	1.8	1.0
C_4	35.8	35.6	151.9	6.7	11.5	178.8	0.16	116.8	10.9	174.7
	10.2	10.0	3.3	1.0	0.9	3.4	0.14	7.6	1.1	2.8
C_5	4.1	4.1	8.8	3.9	2.5	6.9	0.01	9.9	5.3	6.8
	0.8	0.8	1.3	0.6	0.6	0.9	0.01	1.4	0.7	0.9

Table 6. Standard errors in pixels for W_2

	Points									
Pattern	1	2	3	4	5	6	1-2	1-3	4-5	4-6
C_1	3.5	3.4	4.2	3.2	2.1	3.4	0.01	5.6	4.3	4.3
	1.1	1.1	1.8	1.0	1.4	1.7	0.01	1.3	0.7	1.1
C_2	5.1	5.0	6.1	4.1	3.4	4.9	0.01	7.9	5.7	6.2
	1.3	1.3	2.2	1.1	1.7	2.0	0.01	1.8	1.0	1.4
C_3	13.8	13.8	11.4	6.5	35.6	6.6	0.02	23.5	40.8	10.7
	1.6	1.6	6.5	1.4	1.8	2.1	0.02	6.2	1.8	1.4
C_4	41.6	41.4	176.2	6.8	13.2	208.1	0.19	135.2	12.6	204.4
	11.6	11.4	3.9	1.5	1.9	4.6	0.16	8.8	1.4	3.5
C_5	4.1	4.1	9.0	4.5	2.6	7.0	0.01	10.0	5.9	7.2
	1.1	1.1	2.3	1.1	1.7	2.0	0.01	1.8	1.0	1.4

Table 7. Standard errors in pixels for W_3

	Points									
Pattern	1	2	3	4	5	6	1-2	1-3	4-5	4-6
C_1	3.5	3.5	4.4	3.3	2.1	3.4	0.01	5.8	4.4	4.5
	1.2	1.2	2.6	0.2	1.7	2.8	0.01	2.2	1.0	2.3
C_2	5.1	5.1	6.4	4.2	3.4	5.0	0.01	8.2	5.8	6.4
	1.4	1.4	3.2	1.4	2.3	3.3	0.01	2.7	1.3	2.6
C_3	14.4	14.3	11.8	6.5	37.3	6.7	0.02	24.5	42.3	10.8
	1.7	1.7	7.2	1.9	2.2	3.5	0.02	7.8	1.9	2.5
C_4	54.0	53.7	225.6	7.0	17.4	268.0	0.25	172.2	16.1	264.4
	14.9	14.7	5.3	1.7	2.4	5.7	0.21	10.6	1.6	4.5
C_5	4.1	4.1	9.1	4.7	2.6	7.0	0.01	10.2	6.2	7.4
	1.3	1.3	3.2	1.3	2.2	3.1	0.01	2.7	1.3	2.5

Table 8. Standard errors in pixels for W_4

	Points									
Pattern	1	2	3	4	5	6	1-2	1-3	4-5	4-6
C_1	3.5	3.5	4.6	3.3	2.2	3.6	0.01	5.9	4.5	4.6
	1.2	1.2	4.2	1.2	2.2	4.8	0.01	3.9	1.6	4.5
C_2	5.1	5.1	6.7	4.2	3.4	5.1	0.01	8.5	5.9	6.6
	1.5	1.5	4.9	1.6	2.9	5.4	0.01	4.4	1.9	4.8
C_3	14.6	14.6	12.0	6.5	37.9	6.8	0.02	24.8	42.9	10.9
	1.8	1.8	9.0	2.9	3.2	6.2	0.02	9.5	2.4	4.7
C_4	86.0	85.6	353.9	7.5	28.3	423.2	0.41	268.3	25.3	418.8
	23.6	23.2	5.7	1.8	2.9	7.7	0.33	14.5	2.1	6.7
C_5	4.2	4.2	9.3	4.8	2.7	7.1	0.01	10.4	6.3	7.6
	1.4	1.4	4.8	1.5	2.8	5.1	0.01	4.3	1.9	4.6

DISCUSSION

The expected DTM horizontal standard errors owing to imprecision in the exterior orientation estimates are summarized in figures 2 through 6. Note that the results are presented in terms of the Landsat foot print dimension (79 meters) and that the results pertain to a standard error of one line and one sample in the DTM point identification.

Except for the C_4 results, the along-track errors (σ_e) do not vary greatly as the exterior orientation position parameter weights vary. The across-track errors (σ_s) do vary, but are small with respect to the along-track errors. One reason for the noticeable increase in error for C_4 as the weights decrease is that there was only 1 degree of freedom associated with the C_4 adjustment. Patterns C_1, C_2, and C_3 are similar in that the control points are symmetrically distributed over the Landsat format. The along-track errors for C_1 and C_2 approximate the $\sqrt{N}$ law of least-square averages; whereas, there is little difference in the across-track error. The C_3 error results increase considerably from C_2 because there are only 3 degrees of freedom associated with the adjustment. Finally, there are more degrees of freedom associated with C_5 (25) than with C_2 (13), yet the error estimates are larger. The reason for this is that there were no observations along the vehicle ground track for C_5.

In order to lower the horizontal intersection errors, either more points must be identified and measured or independent observations on the attitude parameters must be obtained. A considerable effort must be expended if the horizontal errors are to be reduced without some additional control in the attitude parameters. Let σ_m be the measuring and identification Landsat error, expressed in pixels, associated with the initial DTM point identification. Using the C_1 results as a base, the following approximation can be used to estimate the expected standard error in the along-track horizontal intersection error:

$$\sqrt{\frac{180}{2N-9}}\ \sigma_M < \sigma_e < \sqrt{\frac{720}{2N-9}}\ \sigma_M$$

N = Number of control points.

For example, if N=95 and if the points are symmetrically scattered over the Landsat format, then $\sigma_m \leq \sigma_e \leq 2\sigma_m$, i.e., the along-track intersection standard error is between 80 and 160 meters. This result pertains to a point identification and measuring error of 1 pixel, which is unrealistic. Note that identification errors can easily assign the measurement to the next swath, which is a time error of 0.07342 second or 6 pixels.

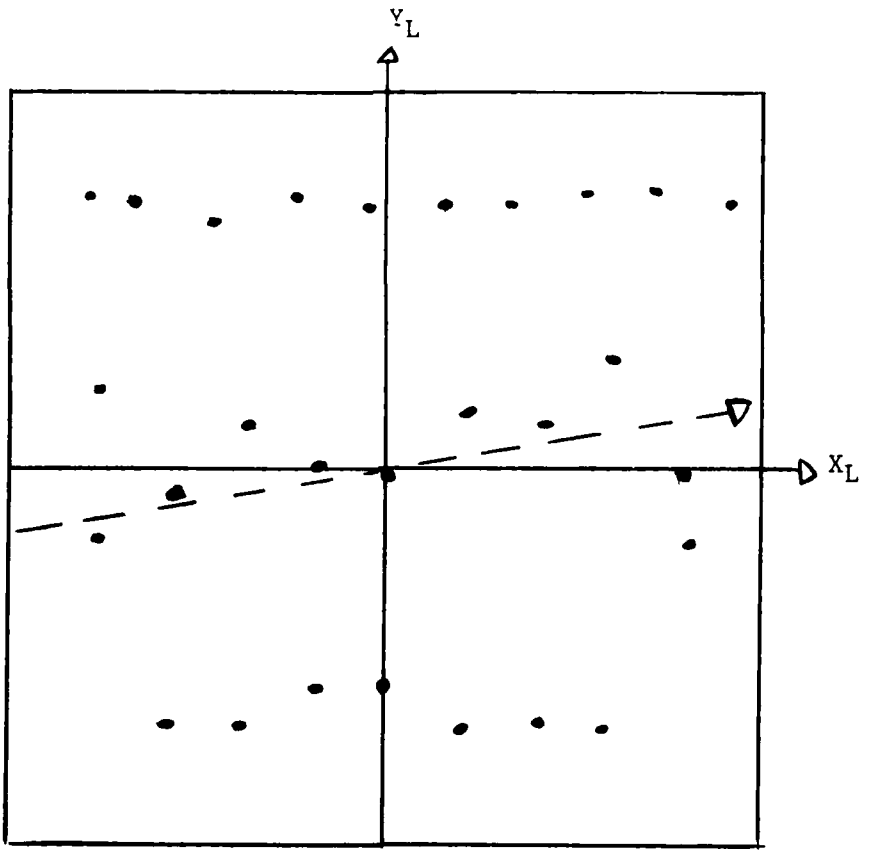

Control Point Pattern for C_1

Weight	Absolute	Relative
W_1	$2 = \sigma_e \leq 4$	$0 \leq \sigma_e \leq 5$
	$\sigma_s \leq 1$	$0 \leq \sigma_s \leq 1$
W_2	$2 \leq \sigma_e \leq 4$	$0 \leq \sigma_e \leq 6$
	$1 \leq \sigma_s \leq 2$	$0 \leq \sigma_s \leq 1$
W_3	$2 \leq \sigma_e \leq 4$	$o \leq \sigma_e \leq 6$
	$1 \leq \sigma_s \leq 3$	$0 \leq \sigma_s \leq 2$
W_4	$2 \leq \sigma_e \leq 5$	$0 \leq \sigma_e \leq 6$
	$1 \leq \sigma_s \leq 5$	$0 \leq \sigma_s \leq 5$

Figure 2. Error summary for C_1.

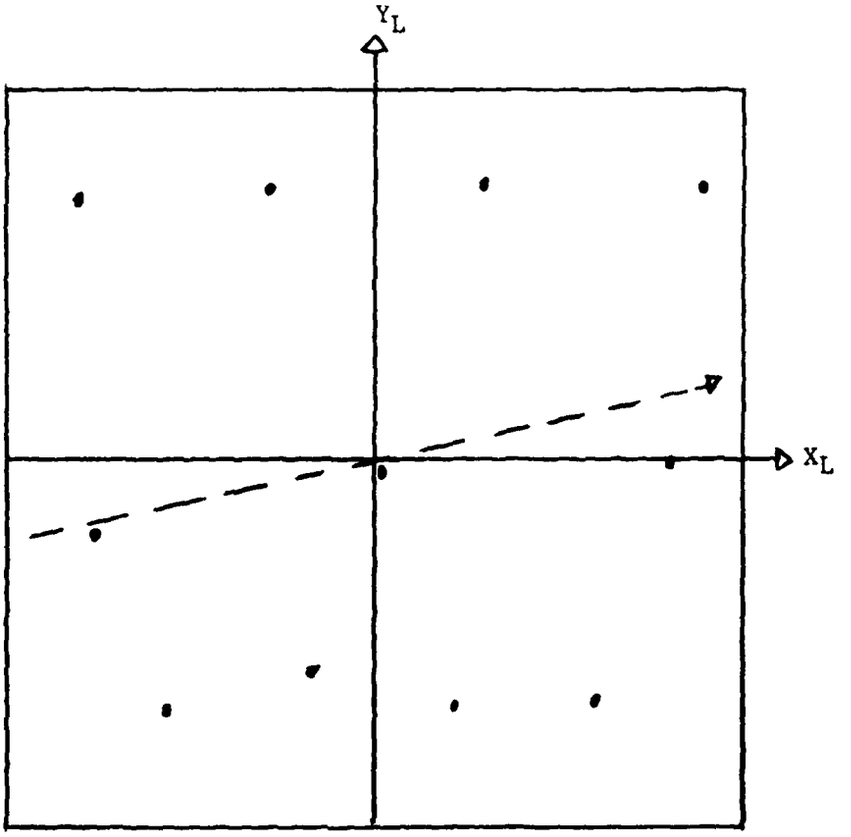

Control Point Pattern for C_2

Weight	Absolute	Relative
W_1	$3 \leq \sigma_e \leq 4$	$0 \leq \sigma_e \leq 8$
	$\sigma_s \leq 1$	$0 \leq \sigma_s \leq 1$
W_2	$3 \leq \sigma_e \leq 6$	$0 \leq \sigma_e \leq 8$
	$1 \leq \sigma_s \leq 2$	$0 \leq \sigma_s \leq 2$
W_3	$3 \leq \sigma_e \leq 6$	$0 \leq \sigma_e \leq 8$
	$1 \leq \sigma_s \leq 3$	$0 \leq \sigma_s \leq 3$
W_4	$3 \leq \sigma_e \leq 7$	$0 \leq \sigma_e \leq 10$
	$2 \leq \sigma_s \leq 5$	$0 \leq \sigma_s \leq 5$

Figure 3. Error summary for C_2.

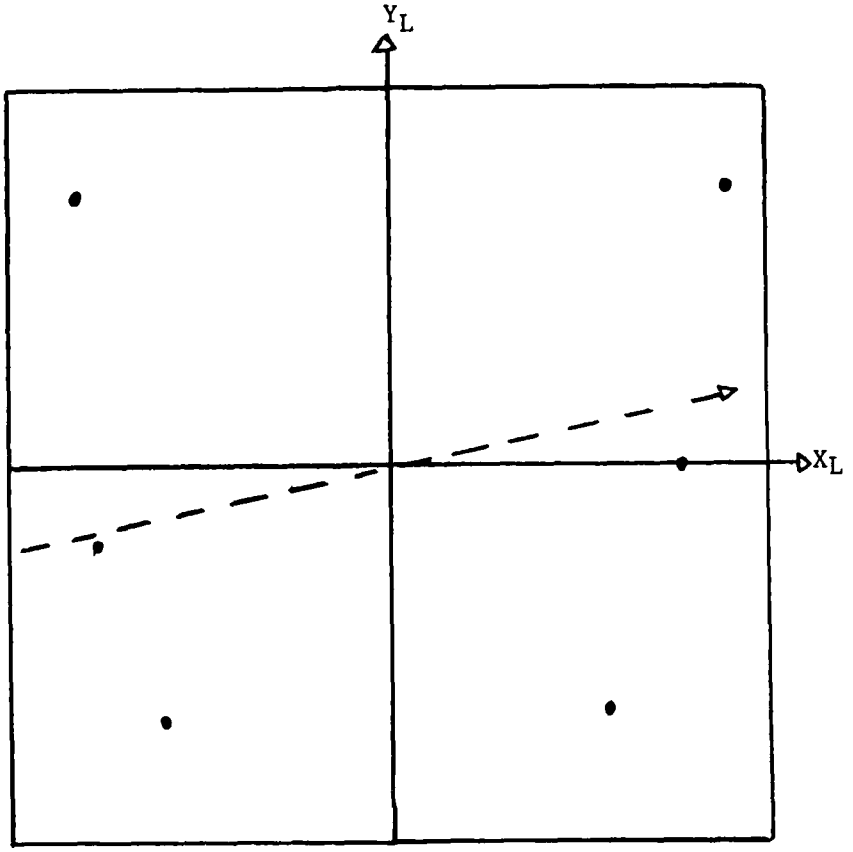

Control Point Pattern for C_3

Weight	Absolute	Relative
W_1	$7 \leq \sigma_e \leq 32$	$0 \leq \sigma_e \leq 37$
	$1 \leq \sigma_s \leq 6$	$0 \leq \sigma_s \leq 6$
W_2	$7 \leq \sigma_e \leq 36$	$0 \leq \sigma_e \leq 41$
	$1 \leq \sigma_s \leq 7$	$0 \leq \sigma_s \leq 6$
W_3	$7 \leq \sigma_e \leq 37$	$0 \leq \sigma_e \leq 42$
	$2 \leq \sigma_s \leq 7$	$0 \leq \sigma_s \leq 8$
W_4	$7 \leq \sigma_e \leq 38$	$0 \leq \sigma_e \leq 43$
	$2 \leq \sigma_s \leq 9$	$0 \leq \sigma_s \leq 10$

Figure 4. Error summary for C_3.

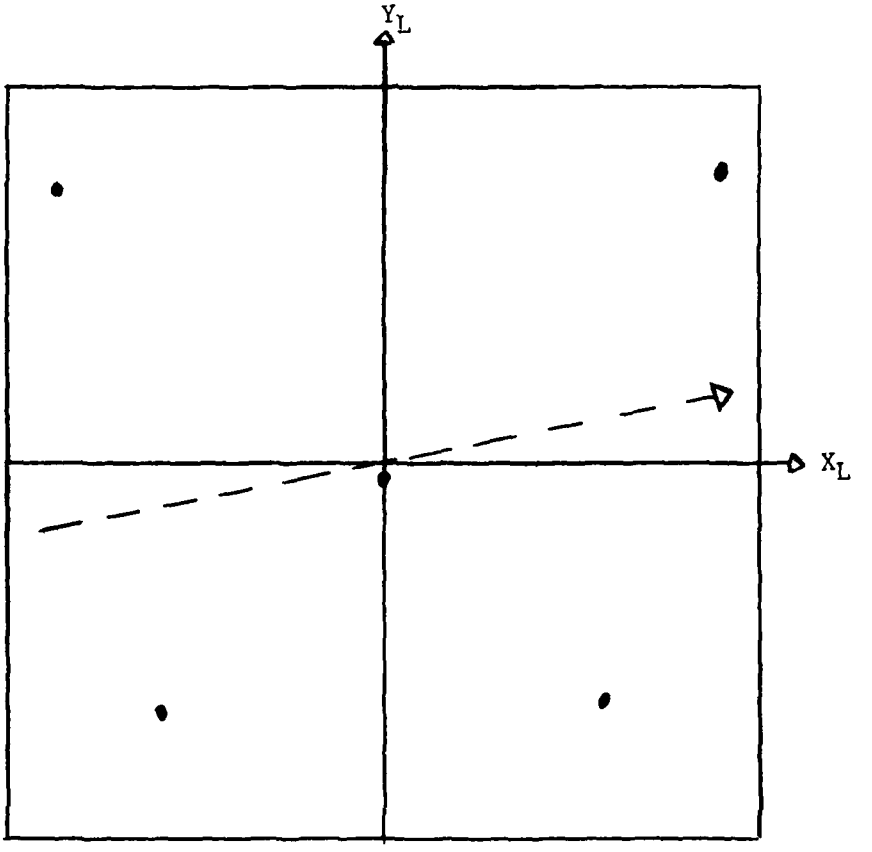

Control Point Pattern for C_4

Weight	Absolute	Relative
W_1	$7 \leq \sigma_e \leq 179$	$0 \leq \sigma_e \leq 175$
	$1 \leq \sigma_s \leq 10$	$0 \leq \sigma_s \leq 8$
W_2	$7 \leq \sigma_e \leq 208$	$0 \leq \sigma_e \leq 204$
	$2 \leq \sigma_s \leq 12$	$0 \leq \sigma_s \leq 9$
W_3	$7 \leq \sigma_e \leq 268$	$0 \leq \sigma_e \leq 264$
	$2 \leq \sigma_s \leq 15$	$0 \leq \sigma_s \leq 11$
W_4	$8 \leq \sigma_e \leq 423$	$0 \leq \sigma_e \leq 419$
	$2 \leq \sigma_s \leq 24$	$0 \leq \sigma_s \leq 15$

Figure 5. Error summary for C_4.

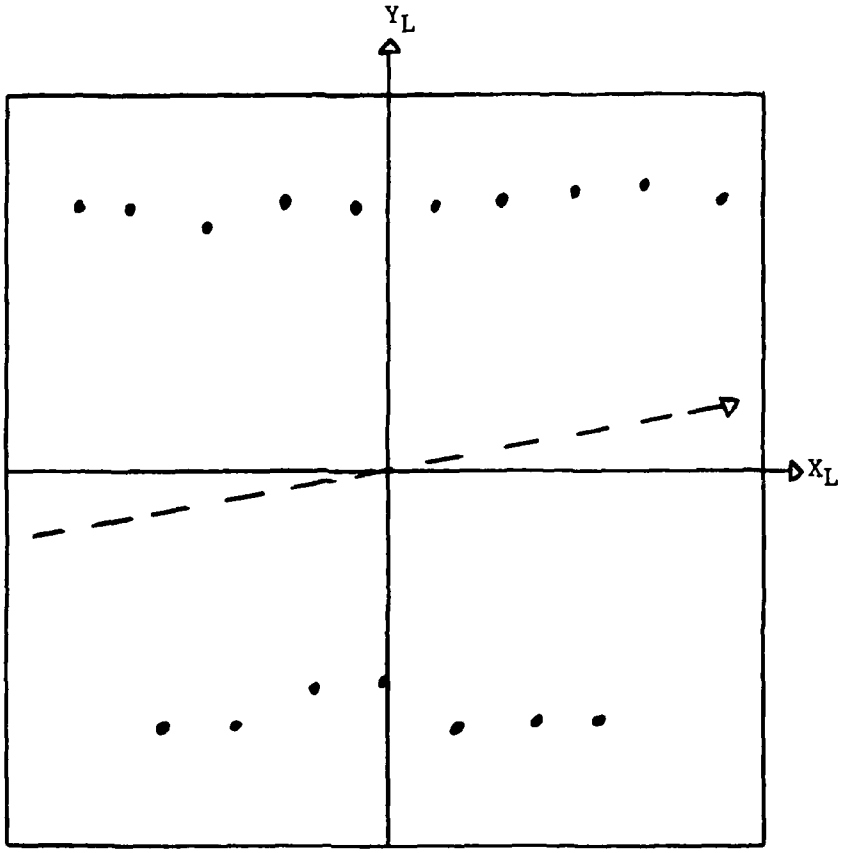

Control Point Pattern for C_5

Weight	Absolute	Relative
W_1	$3 \leq \sigma_e \leq 9$	$0 \leq \sigma_e \leq 10$
	$\sigma_s \leq 1$	$0 \leq \sigma_s \leq 1$
W_2	$3 \leq \sigma_e \leq 9$	$0 \leq \sigma_e \leq 10$
	$1 \leq \sigma_s \leq 2$	$0 \leq \sigma_s \leq 2$
W_3	$3 \leq \sigma_e \leq 9$	$0 \leq \sigma_e \leq 10$
	$1 \leq \sigma_s \leq 3$	$0 \leq \sigma_s \leq 3$
W_4	$3 \leq \sigma_e \leq 9$	$0 \leq \sigma_e \leq 10$
	$1 \leq \sigma_s \leq 5$	$0 \leq \sigma_s \leq 5$

Figure 6. Error summary for C_5.

The technique described above and in appendix E is one way to relate a Landsat image to a DTM. It is difficult to believe that enough points can be accurately defined and measured on both of the soft copy representations to precisely determine the exterior orientation of the scanning vehicle in the DTM coordinate frame. Consider figures 7 and 8. Figure 7 represents a gray shade subscene derived from a DTM, which in turn was produced by DMA from 1:250,000 scale maps. The horizontal ground spacing of the DTM is 64 meters. Figure 8 is a corresponding Landsat subscene. It seems unlikely that the procedure will work in this situation. It is true that the area is relatively flat. Figure 9 is another gray shade relief (and of another region) where topographic detail is more obvious and more readily identified.

If points are identified on maps and on Landsat and if a DTM is intersected to complete the rectification, then there will be the additional concern of the distortion and imprecision between the DTM and the map. Considering the expense and likelihood of an accurate registration, perhaps it should be shown beforehand that the addition of terrain elevation information to the pattern recognition exercise will be worth the effort.

It appears that the full point-by-point rectification as described in appendix A will be an expensive and time-consuming effort, especially if the absolute and relative errors are to be held to about 5 pixels (400 meters). Perhaps a more practical approach would be to intersect the DTM using a regular pattern of Landsat pixels and then to contour the resultant pattern, which could then be easily displayed on the Landsat soft copy.

CONCLUSIONS

1. The exterior orientation of a Landsat exposure can be accurately represented by quadratic time polynomials for each of the six parameters.

2. The technique of determining corresponding points between a Landsat image and a gray shade relief image is not feasible over the relatively flat terrain used in this study.

3. The utility of terrain elevation information in pattern recognition should be demonstrated before the rectification procedure described in this report is used.

Figure 7. Gray shade example.

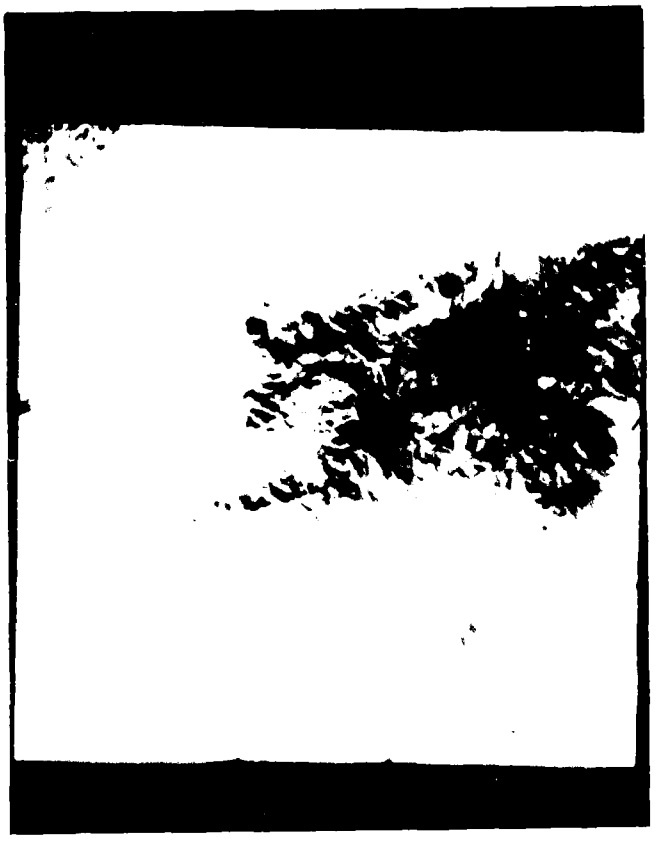

Figure 8. LANDSAT subscene.

Figure 9. Gray shade example.

APPENDIX A. LANDSAT INTERSECTION MODEL

Consider figure A1. Coordinates for an arbitrary ground point P in (G) are calculated from the vector equation $\bar{P} = \bar{V} + \bar{D}$, where (G) is a local ground coordinate frame. The vector $\bar{V}$ represents the position of the vehicle at exposure time of P, and $\bar{D}$ represents the vector from V to P at exposure time.

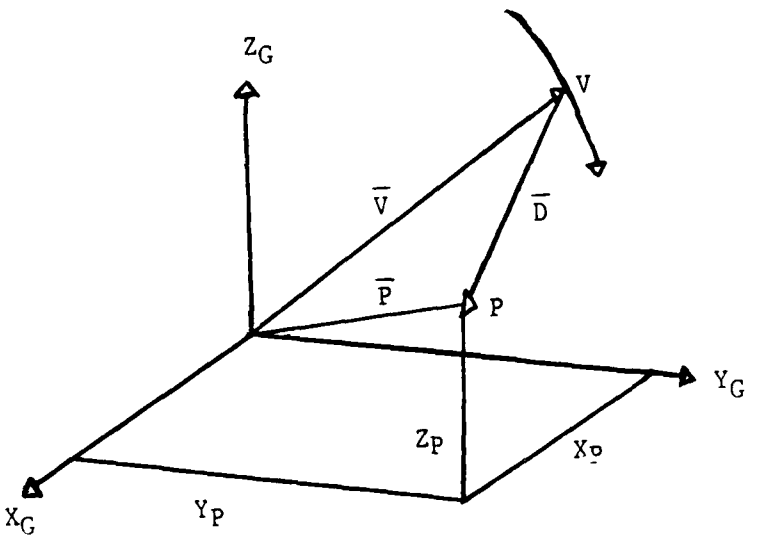

Figure A1. Intersection geometry.

The ground coordinates of P are written as follows:

$$\begin{pmatrix} X_P \\ Y_P \\ Z_P \end{pmatrix}_{IJK} = \begin{pmatrix} X_V \\ Y_V \\ Z_V \end{pmatrix}_{JK} + d_{IJK} M^T_{GV_{JK}} \begin{pmatrix} \alpha_p \\ \beta_p \\ \gamma_p \end{pmatrix}_{IJ} \qquad (A1)$$

where

I=1,6	:	Specific line within Kth swath
J	:	Sample value along a line
K	:	Specific swath in which P was imaged
d_{ITK}	:	Distance between P and V at exposure time
$(\alpha_P, \beta_P, \gamma_P)$	:	Direction cosines of imaging ray in vehicle reference frame (V)
$M_{GV_{JK}}$	:	Rotation matrix relating (G) to (V) at exposure time

The swath notation is necessary since Landsat collects data simultaneously along six parallel lines. The subscripts I, J, and K define which of the basic measurements have a bearing on the particular calculation.

The camera for any one of the four multispectral bands can be represented by a simple linear array (see figure A2) in the focal plane. An oscillating flat mirror scans in such a manner that imagery moves across the array in the y-direction, while the vehicle carries the scanner along in the x-direction. A line of imagery moves across the four arrays where a given wavelength is sampled at each array. The detectors are sampled so that the six corresponding points from band to band are equally spaced in time. Except for a negligible image motion, the four spectral values for any one of the six pixels pertain to the same ground foot print.

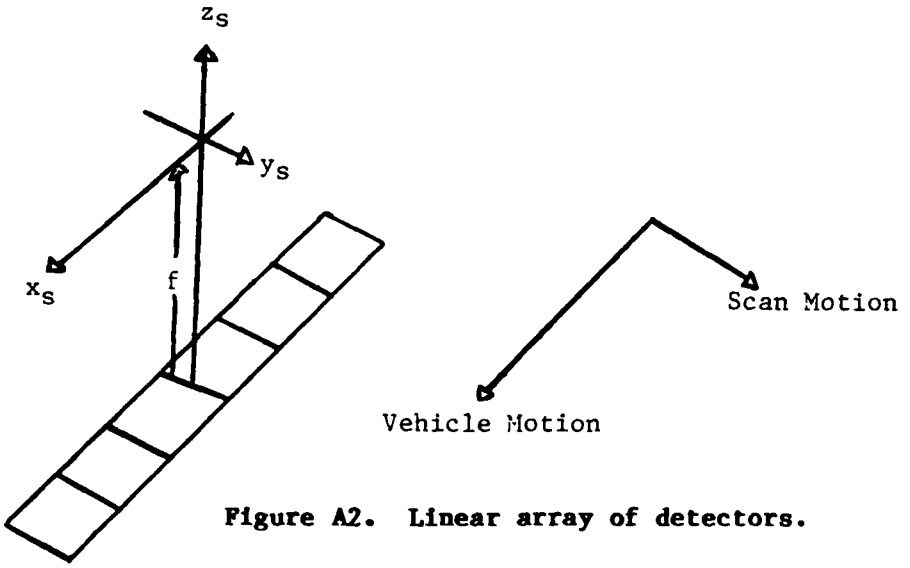

Figure A2. Linear array of detectors.

The intersection model expressed by equation 1 pertains to any one of the four spectral bands and, in fact, to a composite image derived from two or more of the spectral bands. This is true because the corresponding foot prints are, except for image motion, identical. Let figure A2 represent the instantaneous array of detectors for a specific band, or for a particular composite. The scanner coordinates for the I^{th} point are

$$\begin{pmatrix} x_I \\ 0 \\ -f \end{pmatrix} 1/\ell_I = \begin{pmatrix} \sin \gamma_I \\ 0 \\ -\cos \gamma_I \end{pmatrix} \tag{A2}$$

where

$$\ell_I = \sqrt{x_I^2 + f^2}$$

The six discrete values can be computed directly from the focal length and from the detector dimensions. For example, the focal length for Landsat 2 is 32.34 inches and for each detector is 71 μm by 71 μm.

The remaining model parameters are described in figure A3. The vehicle reference frame (V) is nominally oriented so that Z_V is normal to the earth's surface and so that X_V is tangent to the flight path. The three fundamental angles used to define M_{GV} will be modeled as time polynomials. For example, if the fundamental angles are roll (w), pitch (ϕ), and yaw (K), then

$$\begin{pmatrix} w \\ \phi \\ K \end{pmatrix}_{JK} = B_N T \tag{A3}$$

where

$T_N T = (1, t_{JK}, t^2{}_{JK}, \ldots, t^N{}_{JK})$

$t_{JK} = T_{JK} - T_o$

T_{JK} : Exposure time

T_o : Arbitrary epoch time

B : 3X(N+1) matrix of attitude constants

N : Order of time polynomial

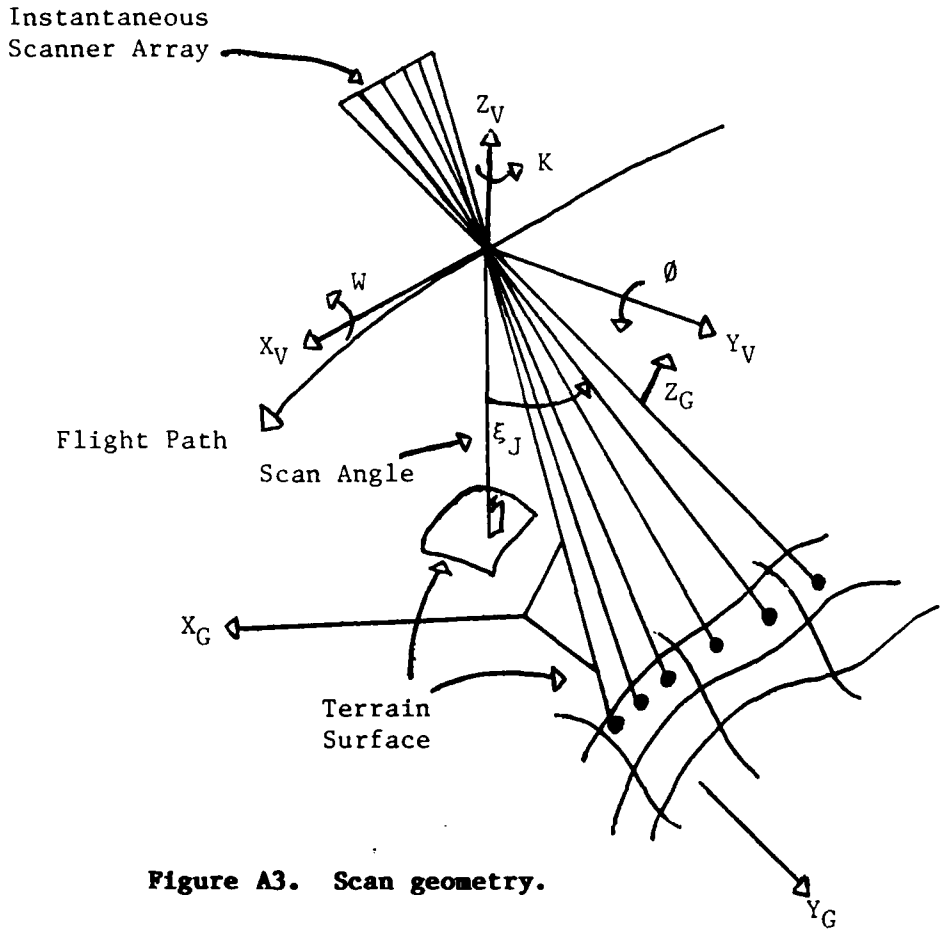

Figure A3. Scan geometry.

Vehicle positions will also be represented by time polynomials.

$$\begin{pmatrix} X_V \\ Y_V \\ Z_V \end{pmatrix}_{JK} = AT_M \qquad \text{(A4)}$$

where

A : 3X(M+1) matrix of position constants

M : Order of time polynomial

The direction cosines of the imaging ray in (V) are derived from the scanner coordinates and from M_{SV_J}, the rotation matrix relating the oscillating flat mirror to (V). From figure A3,

$$M_{SV_J} = \begin{pmatrix} 1 & 0 & 0 \\ 0 & \text{Cos } \xi_J & -\text{Sin } \xi_J \\ 0 & \text{Sin } \xi_J & \text{Cos } \xi_J \end{pmatrix} \tag{A5}$$

where ξ_J is the scan angle.

Then, the direction cosines of the imaging array in (V) are

$$\begin{pmatrix} \alpha_P \\ \beta_P \\ \gamma_P \end{pmatrix}_{IJ} = M_{SV_J} \begin{pmatrix} \text{Sin } \gamma_I \\ 0 \\ -\text{Cos } \gamma_I \end{pmatrix} \begin{pmatrix} \text{Sin } \gamma_I & \\ \text{Sin } \xi_J & \text{Cos } \gamma_I \\ -\text{Cos } \xi_J & \text{Cos } \gamma_I \end{pmatrix} \tag{A6}$$

The coordinates of P in (G) can be calculated from a Landsat image, providing the following quantities are known or can be computed:

A and B	:	3(M+N+2) exterior orientation constants
T_{JK}	:	Exposure time
ξ_J	:	Scan angle
γ_I	:	Array measurement
d_{IJK}	:	Slant range distance between the vehicle and P at exposure time.

The exterior orientation constants are determined by a least-squares adjustment (see appendix B). Exposure time is computed as follows:

$$T_{JK} = T_1 + (K-1)\Delta T + \left(\frac{J-1}{N_{P-1}}\right) \delta T$$

where

T_1 : Time of start of first swath

ΔT : Scan time, plus return time

K : Swath number

δT : Scan time

J : Sample number

N_P : Total number of samples per line

The scan angle is computed in the following way:

$$\xi_J = \xi_F + \left(\frac{J-1}{N_{P-1}}\right) (\xi_L - \xi_F)$$

where

ξ_F : Scan angle for J=1

ξ_L : Scan angle for J=NP

The following values were used in Landsat 2:

ΔT = 0.07342 seconds

δT = 0.033 seconds

ξ_F = -5.8 degrees

ξ_L = +5.8 degrees

The slant range distance d_{IJK} can be calculated only if additonal information about the terrain is provided, a DTM for example. Rewrite equation (A1) and drop the subscripts I, J, and K,

$$\begin{pmatrix} X_P \\ Y_P \\ Z_P \end{pmatrix} = \begin{pmatrix} X_V \\ Y_V \\ Z_V \end{pmatrix} + d \begin{pmatrix} \lambda_P \\ \varepsilon_P \\ \mu_P \end{pmatrix} \qquad \text{(A7)}$$

where

$$(\lambda_P, \varepsilon_P, \mu_P) = (\alpha_P, \beta_P, \gamma_P)M_{GV_P}$$

Suppose a good estimate of Z_P, say Z_{P_o}, exists, then from equation (A7)

$$d_o = (Z_{P_o} - Z_V)\mu_P$$

and

$$X_{P_o} = X_V + d_o\lambda_P$$
$$Y_{P_o} = Y_V + d_o\varepsilon_P$$

An improved value of Z_P can be obtained by interpolating in the DTM. Consider figure A4.

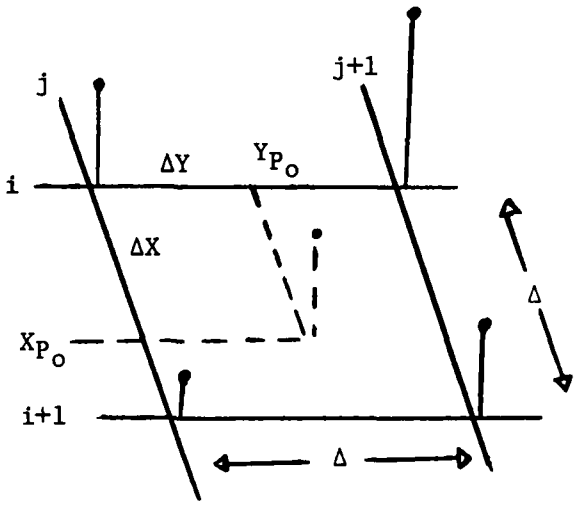

Figure A4. Bilinear interpolation.

Bilinear interpolation for Z_{P_1} produces the following values:

$$Z_{P_1} = Z_A + \delta_X(Z_B - Z_A)$$

$$Z_A = Z(i,j) + \delta_Y[Z(i,j+1) - Z(i,j)]$$

$$Z_B = Z(i+1,j) + \delta_Y[Z(i+1,j+1) - Z(i+1,j)]$$

$$\delta_X = \Delta X/\Delta$$

$$\delta_Y = \Delta Y/\Delta$$

Δ : Horizontal spacing of DTM

If $|Z_{P_o} - Z_{P_1}| \leq \ell$, a preselected value, then $Z_P = Z_{P_1}$. If the convergence criterion is not met, then repeat the process using $d_1 = (Z_{P_1} - Z_V)/\mu_p$ and associated values for X_{P_1} and Y_{P_1}.

Line of sight should not be a problem here. Consider figure A5.

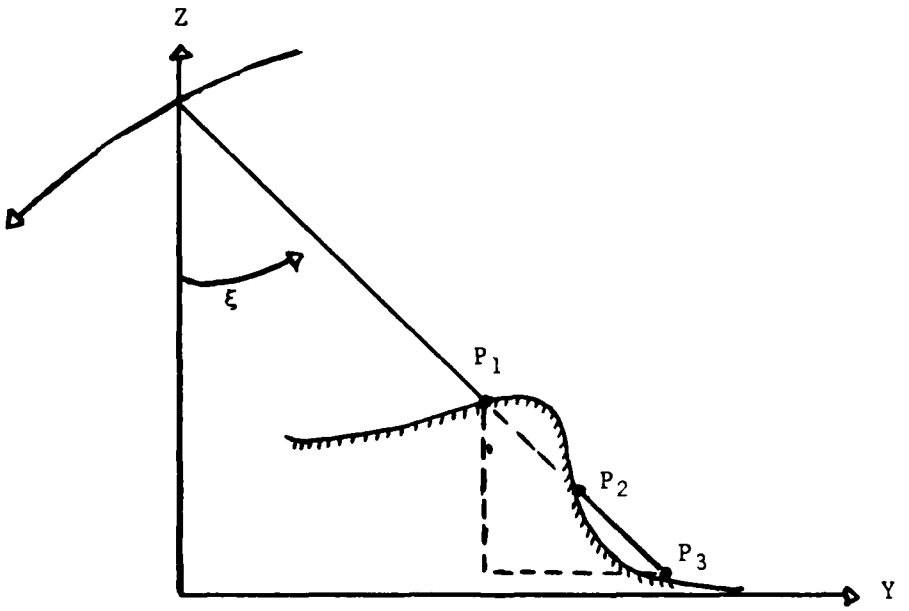

Figure A5. Line of sight.

Either P_1, P_2, or P_3 would satisfy the iterative process, depending on the initial estimate Z_{P_o}. From the diagram Tan $\xi = \Delta Y/\Delta Z$, or

$$\Delta Z = \Delta Y/\text{Tan } \xi \geq 9.845\ \Delta Y$$

Since $|\xi| < 5.8$ degrees

Line of sight is obscured if the change in elevation ΔZ exceeds 9.845 ΔY. The minimum Y-spacing for a DTM derived from 1:250,000 scale maps is 208.3 feet (65 meters), which says that ΔZ must change by at least 2051 feet (650 meters) over the horizontal spacing before line of sight fails.

The number of iterations should be monitored since it is possible, but unlikely, that the process could cycle. Consider figure A6.

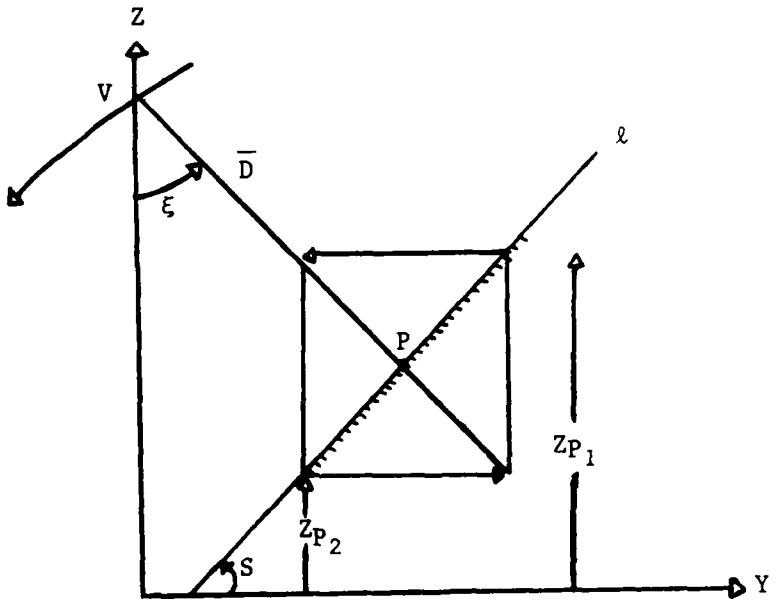

Figure A6. Iterative breakdown.

The process will cycle if the slope at P and along ℓ is $S = 90^o - \xi$. The linear section ℓ is defined by the DTM and by the plane containing the local vertical at V and along the ray $\bar{D}$. Since $|\xi| < 5.8$ degrees, S must be $\geq$ 84.2 degrees for the process to cycle.

APPENDIX B. LEAST-SQUARES ADJUSTMENT OF LANDSAT EXTERIOR ORIENTATION MODEL PARAMETERS

Consider equation (A1). Drop the subscripts I, J, and K, and rewrite the equation as follows:

$$\begin{pmatrix} \alpha_P \\ \beta_P \\ \gamma_P \end{pmatrix} = M_{GV_P} \begin{pmatrix} X_P - X_V \\ Y_P - Y_V \\ Z_P - Z_V \end{pmatrix} 1/d_{PV}$$

Perform the indicated matrix operations, and divide the resulting first and second equations by the third equation to obtain the following condition equations:

$$F = \text{Tan } \gamma \text{ Sec } \xi + \frac{m_{11}(X_P-X_V) + m_{12}(Y_P-Y_V) + m_{13}(Z_P-Z_V)}{m_{31}(X_P-X_V) + m_{32}(Y_P-Y_V) + m_{33}(Z_P-Z_V)} = 0 \qquad \text{(B1)}$$

$$G = \text{Tan } \xi + \frac{m_{21}(X_P-X_V) + m_{22}(Y_P-Y_V) + m_{23}(Z_P-Z_V)}{m_{31}(X_P-X_V) + m_{32}(Y_P-Y_V) + m_{33}(Z_P-Z_V)} = 0 \qquad \text{(B2)}$$

where $(m_{ij};\ i=1,3 \text{ and } j=1,3)$ are the elements of M_{GV_P}.

The expressions F and G are nonlinear in the exterior orientation constants. In order to use the least-squares technique, F and G must be approximated with linear equations. Assume that reasonable estimates of the 3(N+M+2) unknown constants defined in equations (A3) and (A4) exist. Equations (B1) and (B2) will be approximated by the constant and first-order Taylor expansion terms of F and G about the estimates. The approximate equations are linear in corrections to the parameter estimates, and thus the least-squares technique can be used to solve for the corrections.

Represent the condition equations (B1) and (B2) from equation (A1) as

$$F = \mu + R/T = 0$$

$$G = \nu + S/T = 0$$

A straightforward differentiation of F and G with respect to X_V, Y_V, and Z_V produces the following:

$$C_V = \frac{\partial(F,G)}{\partial(X_V,Y_V,Z_V)} = -\frac{1}{T^2} \begin{pmatrix} T & 0 & -R \\ 0 & T & -S \end{pmatrix} M_{GV_P} \qquad \text{(B3)}$$

If the fundamental angles of M_{GV_P} are roll (w), pitch (ϕ), and yaw (K), then a slightly more complicated exercise in partial differentiation produces the following:

$$C_\alpha = \frac{\partial(F, G)}{\partial(w,\phi,K)} = \begin{pmatrix} \frac{\partial F}{\partial w} & \frac{\partial F}{\partial \phi} & \frac{\partial F}{\partial K} \\ \frac{\partial G}{\partial w} & \frac{\partial G}{\partial \phi} & \frac{\partial G}{\partial K} \end{pmatrix} \qquad \text{(B4)}$$

where

$$\frac{\partial F}{\partial K} = S/T \qquad \frac{\partial G}{\partial K} = -R/T$$

$$\frac{\partial F}{\partial \phi} = \text{Sec } \phi \left[T \frac{\partial F}{\partial X_V} + \frac{(X_P - X_V)}{T} \frac{\partial G}{\partial K} \right]$$

$$\frac{\partial G}{\partial \phi} = \text{Sec } \phi \left[T \frac{\partial G}{\partial X_V} - \frac{(X_P - X_V)}{T} \frac{\partial F}{\partial K} \right]$$

$$\frac{\partial F}{\partial w} = (Y_P - Y_V)\frac{\partial F}{\partial Z_V} - (Z_P - Z_V)\frac{\partial F}{\partial Y_V}$$

$$\frac{\partial G}{\partial w} = (Y_P - Y_V)\frac{\partial G}{\partial Z_V} - (Z_P - Z_V)\frac{\partial G}{\partial Y_V}$$

Define the (3 x 3) diagonal matrix E_L where the diagonal elements are (L+1) dimensional row vectors defined as $(1, t_{JK}, t^2_{JK} \ldots, t^L_{JK}) = T^T_L$. Then, from equations (A3) and (A4), the partial derivatives of F and G with respect to the position parameters and with respect to the attitude parameters are $C_V.E_M$ and $C_\alpha.E_N$, respectively. Let ΔA be the 3(M+1) vector of position corrections and let ΔB be the 3(N+1) vector of attitude corrections. The first (M+1) corrections of ΔA pertain to X_V, the next (M+1) corrections pertain to Y_V, and finally the last (M+1) corrections pertain to Z_V. A similar definition holds for ΔB. The "linearized" part of F and G that pertains to the exterior orientation parameter corrections is the following:

$$C_V E_M \Delta A + C_\alpha E_N \Delta B$$

or

$$\begin{bmatrix} C_V E_M, & C_\alpha E_N \end{bmatrix} \begin{pmatrix} \Delta A \\ \Delta B \end{pmatrix}$$

or

$$Q\Delta \qquad (B5)$$

Q : $2x3(M+N+2)$

Δ : $3(M+N+2)x1$

Equations (B1) and (B2) are also nonlinear in the measured data; namely, line (ℓ) and sample (p). The partial derivatives of F and G with respect to ℓ and p are calculated as before by applying the chain rule.

$$\frac{\partial(F,G)}{\partial(\ell,p)} = \frac{\partial(F,G)}{\partial(\xi,\gamma)} \frac{\partial(\xi,\gamma)}{\partial(\ell,p)} + \frac{\partial(F,G)}{\partial(X_V,Y_V,Z_V)} \frac{\partial(X_V,Y_V,Z_V)}{\partial t} \frac{\partial t}{\partial(\ell,p)} + \frac{\partial(F,G)}{\partial(w,\phi,K)} \frac{\partial(w,\phi,K)}{\partial t} \frac{\partial t}{\partial(\ell,p)} \qquad (B6)$$

From equation (B1),

$$\frac{\partial(F,G)}{\partial(\xi,\gamma)} = \begin{pmatrix} \text{Tan } \gamma \text{ Sec } \xi \text{ Tan } \xi & \text{Sec}^2\gamma \text{ Sec } \xi \\ \text{Sec}^2\xi & 0 \end{pmatrix}$$

and from equations (A2) and (A6),

$$\frac{\partial(\xi,\gamma)}{\partial(\ell,p)} = \begin{pmatrix} 0 & (\xi_L - \xi_F) \,/\, (N_{P-1}) \\ \Delta x/f & 0 \end{pmatrix}$$

Δx : line spacing

Define $\dot{T}_L^T = \left(0,\ 1,\ 2t_{JK},\ \ldots,\ Lt_{JK}^{L-1}\right)$ and calculate the following vector quantities:

$$H_V = A\ \dot{T}_M$$

and

$$H_\alpha = B\ \dot{T}_N$$

Then from equations (B3) and (B4)

$$\frac{\partial(F,G)}{\partial(X_V,Y_V,Z_V)} \cdot \frac{\partial(X_V,Y_V,Z_V)}{\partial t} \cdot \frac{\partial t}{\partial(\ell,p)} = C_V \cdot H_V \cdot \frac{\partial t}{\partial(\ell,p)}$$

$$\frac{\partial(F,G)}{\partial(w,\phi,K)} \cdot \frac{\partial(w,\phi,K)}{\partial t} \frac{\partial t}{\partial(\ell,p)} = C_\alpha H_\alpha \cdot \frac{\partial t}{\partial(\ell,p)}$$

where

$$\frac{\partial t}{\partial(\ell,p)} = (\Delta T,\ \delta T/(NP-1))$$

Note that time does not vary over lines within a swath.

Let D represent the (2 x 2) matrix given in equation (B6), and let $(\varepsilon_\ell, \varepsilon_p)$ represent the unknown errors associated with the measured line and sample values. The "linearized" pair of observation equations then are

$$\begin{pmatrix} F \\ G \end{pmatrix} + \quad Q\Delta + D\begin{pmatrix} \varepsilon_\ell \\ \varepsilon_p \end{pmatrix} \sim \begin{pmatrix} 0 \\ 0 \end{pmatrix}$$

The matrix elements as well as F and G are evaluated at the estimated values of the parameters. Let Σ_i be the (2 x 2) covariance matrix associated with i^{th} observational pair, then the i^{th} weight matrix is

$$w_i = \left(D_i \Sigma_i D_i^T \right)^{-1}$$

and the least-squares solution for Δ is

$$\hat{\Delta} = -\left(\sum_{i=1}^{N_o} Q_i^T w_i Q_i \right)^{-1} \left(\sum_{i=1}^{N_o} Q_i^T w_i \begin{pmatrix} F \\ G \end{pmatrix}_i \right)$$

N_o: Number of observations

There are $(2N_o - 3(N+M+2))$ degrees of freedom associated with this adjustment. The residual sum of squares is

$$SS = \sum_{i=1}^{N_o} (F,G)_i \begin{pmatrix} F \\ G \end{pmatrix}_i - \hat{\Delta}^T \left(\sum_{i=1}^{N_o} Q_i^T w_i \begin{pmatrix} F \\ G \end{pmatrix}_i \right)$$

and the covariance matrix associated with the parameter estimates is the following:

$$\sigma_{EX} = \left(\sum_{i=1}^{N_o} Q_i^T w_i Q_i \right)^{-1} \qquad \text{(B7)}$$

APPENDIX C. LANDSAT DATA GENERATOR

Assume that the dynamic model described by equation (A1) is accurate, then if P is known, the exposure time t_p can be determined and the corresponding line (ℓ_p) and sample value (p_p) may be computed from t_p. Rewrite equation (A1) in the following way:

$$\begin{pmatrix} x_I/\ell_I \\ 0 \\ -f/\ell_I \end{pmatrix} = M_{SV_J}^T \, M_{GV_{JK}} \begin{pmatrix} X_P - X_V \\ Y_P - Y_V \\ Z_P - Z_V \end{pmatrix} 1/d_{IJK} \qquad \text{(C1)}$$

Let $M_{SV_J}^T M_{GV_{JK}} = R_{GS_{JK}}$, then if (C1) is expanded, the following equation may be solved for the exposure time $t_P = t_{JK}$. For convenience, drop the I, J, and K subscripts.

$$E(t) = r_{21}(X_P - X_V) + r_{22}(Y_P - Y_V) + r_{23}(Z_P - Z_V) = 0 \qquad \text{(C2)}$$

Note that (r_{21}, r_{22}, r_{23}) is the second row of R_{GS} and is therefore the scanner y-axis expressed in (G).

Suppose that an initial estimate, t_{P_0}, of the exposure time exists, then t_{P_1} given below is a better estimate:

$$t_{P_1} = t_{P_0} - E(t_{P_0})/\dot{E}(t_{P_0})$$

The expression $\dot{E}$ refers to the time derivative of E. The process can be iterated until the correction is insignificant.

The time derivative is calculated in the following way. Rewrite equation (2) in vector format.

$$E(t) = R_2 \cdot L$$

where

$$R_2T = (r_{21}, r_{22}, r_{23})$$

$$L^T = \left[(X_P - X_V), (Y_P - Y_V) (Z_P - Z_V)\right]$$

The time derivative of E then is

$$\dot{E}(t) = \dot{R}_2 \cdot L + R_2 \cdot \dot{L}$$

where

$$\dot{L}^T = (-\dot{X}_V, -\dot{Y}_V, \dot{Z}_V)$$

From equation (A4),

$$(X_V, Y_V, Z_V) = T_M^T A^T$$

then

$$(\dot{X}_V, \dot{Y}_V, \dot{Z}_V) = \dot{T}_M^T A^T$$

where

$$\dot{T}_M^T = (0, 1, 2tp, \ldots, Mt_P^{M-1})$$

The time derivative of the vector R_2 can be computed in a similar manner. From equation (A5) and equation (B1),

$$R_2 = \begin{pmatrix} m_{21} & m_{31} \\ m_{22} & m_{32} \\ m_{23} & m_{33} \end{pmatrix} \quad \begin{pmatrix} \text{Cos } \xi_P \\ \text{Sin } \xi_P \end{pmatrix}$$

and

$$R_2 = \begin{pmatrix} \dot{m}_{21} & \dot{m}_{31} \\ \dot{m}_{22} & \dot{m}_{32} \\ \dot{m}_{23} & \dot{m}_{33} \end{pmatrix} \begin{pmatrix} \text{Cos } \xi_P \\ \text{Sin } \xi_P \end{pmatrix} + \begin{pmatrix} m_{21} & m_{31} \\ m_{22} & m_{32} \\ m_{23} & m_{33} \end{pmatrix} \begin{pmatrix} -\text{Sin } \xi_P \\ \text{Cos } \xi_P \end{pmatrix} \dot{\xi}_P$$

$$\dot{\xi}_P = (\xi_L - \xi_F)/\delta_T$$

$$\xi_P = \xi_F + \dot{\xi}_P (t_P - t_{1K})$$

T_{1K} : Start time of K^{th} swath.

The time derivatives of the 6 m_{ij} are obtained by a straightforward differentiation of the elements with respect to time.

$$\begin{pmatrix} \dot{m}_{21} \\ \dot{m}_{22} \\ \dot{m}_{23} \end{pmatrix} = \begin{pmatrix} 0 & m_{31} \text{ Sin K} & -m_{11} \\ -m_{23} & m_{32} \text{ Sin K} & -m_{12} \\ m_{22} & m_{33} \text{ Sin K} & -m_{13} \end{pmatrix} \begin{pmatrix} \dot{w} \\ \dot{\phi} \\ \dot{K} \end{pmatrix}$$

$$\begin{pmatrix} \dot{m}_{31} \\ \dot{m}_{32} \\ \dot{m}_{33} \end{pmatrix} = \begin{pmatrix} 0 & \text{Cos } \phi & 0 \\ -m_{33} & m_{31} \text{ Sin w} & 0 \\ m_{32} & -m_{31} \text{ Cos w} & 0 \end{pmatrix} \begin{pmatrix} \dot{w} \\ \dot{\phi} \\ \dot{K} \end{pmatrix}$$

From equation (A3),

$$(w,\phi,K) = T_N^T \; B^T$$

then

$$(\dot{w},\dot{\phi},\dot{K}) = \dot{T}_N^T \; B^T$$

Recall from appendix A that six sample values are collected simultaneously over a swath and that x_I identifies the specific line within a swath. From equation (C1),

$$x_I/\ell_I = R_1 \cdot L/d = \alpha$$

where

R_1 is the first row of R_{GS}

Then $x_I = f\alpha/\sqrt{1-\alpha^2}$, where if f is given in micrometers

$$-3 \leq x_I/71 \leq 3$$

The line number within the swath is the nearest integer associated with $x_I/71$. The sample number is the nearest integer associated with the following expression.

$$J = \frac{(t_p - t_1 - (K-1)\Delta T)(NP-1)}{\delta T} + 1$$

The swath number K must satisfy the following relation:

$$K-1 \leq (t_p - t_1)/\Delta T \leq K$$

Note that the initial estimate $^{T}P_0$ must be within the correct swath time limits. Since the sweep is normal to the vehicle path, an estimate of the exposure time can be obtained by solving the following equation for time:

$$G(T) = \dot{X}_V(X_P-X_V) + \dot{Y}_V(Y_P-Y_V) + \dot{Z}_V(Z_P-Z_V) = 0$$

This equation can be solved for ${}^tP_0$ in a manner similar to the solution of E. In this case, the midtime of the imaging event, say t_{00}, can be used as a first estimate. An improved estimate is

$$t_{01} = t_{00} - G(T_{00})/\dot{G}(T_{00})$$

where

$$\dot{G}(T) = \ddot{X}_V(X_P-X_V) + \ddot{Y}_V(Y_P-Y_V) + \ddot{Z}_V(Z_P-Z_V) - (\dot{X}_V^2 + \dot{Y}_V^2 + \dot{Z}_V^2)$$

where

$$(\ddot{X}_V, \ddot{Y}_V, \ddot{Z}_V) = \ddot{\lambda}^T A^T$$

$$\ddot{\lambda}^T = \left(0,\ 0,\ 2,\ 6t_p,\ 12t_p^2,\ \ldots,\ M(M-1)t_p^{M-2}\right)$$

APPENDIX D. TWO-POINT ERROR PROPAGATION

Consider the intersection equations expressed by equation (A1). The objective here is to propagate position and attitude model errors into a 6 x 6 convariance matrix for two points P_1 and P_2. The right side of equation (A1) must be differentiated with respect to the 3(M+1) position parameters ΔA and with respect to the 3(N+1) attitude parameters ΔB.

$$\frac{\partial(X_P,Y_P,Z_P)}{\partial A} = \frac{\partial(X_P,Y_P,Z_P)}{\partial(X_V,Y_V,Z_V)} \cdot \frac{\partial(X_V,Y_V,Z_V)}{\partial A}$$

$$+ \frac{\partial(X_P,Y_P,Z_P)}{\partial dP} \frac{\partial d_P}{\partial(X_V,Y_V,Z_V)} \frac{\partial(X_V,Y_V,Z_V)}{\partial A}$$

From equation (A1),

$$\frac{\partial(X_P,Y_P,Z_P)}{\partial(X_V,Y_V,Z_V)} = I_3$$

and

$$\frac{\partial(X_P,Y_P,Z_P)}{\partial dP} = M_{GV}^T \begin{pmatrix} \alpha_P \\ \beta_P \\ \gamma_P \end{pmatrix}$$

Since $d_P = \left[(X_P-X_V)^2 + (Y_P-Y_V)^2 + (Z_P-Z_V)^2\right]^{1/2}$, then

$$\frac{\partial d_P}{\partial(X_V,Y_V,Z_V)} = -\left[(X_P-X_V),\ (Y_P-Y_V),\ (Z_P-Z_V)\right]/d_P$$

$$= -(\alpha_P,\beta_P,\gamma_P)M_{GV}$$

Finally, from the discussion in appendix B concerning equation (A4),

$$\frac{\partial(X_V,Y_V,Z_V)}{\partial A} = E_M$$

and collecting terms

$$\frac{\partial(X_P,Y_P,Z_P)}{\partial A} = \left[I_3 - M_{GV}^T \begin{pmatrix}\alpha_P\\ \beta_P\\ \gamma_P\end{pmatrix} (\alpha_P,\beta_P,\gamma_P)M_{GV} \right] E_M \qquad \text{(D1)}$$

The partial derivatives of the intersection equation with respect to the attitude parameters are computed as follows:

$$\frac{\partial(X_P,Y_P,Z_P)}{\partial B} = \frac{\partial(X_P,Y_P,Z_P)}{\partial(w,\phi,K)} \quad \frac{\partial(w,\phi,K)}{\partial B}$$

The (3 x 3) Jacobian $\partial(X_P,Y_P,Z_P)/\partial(w,\phi,K)$ can be evaluated by rewriting equation (A1) in the following way:

$$X_P = X_V + d_P\, C_1.\Psi$$

$$Y_P = Y_V + d_P\, C_2.\Psi$$

$$Z_P = Z_V + d_P\, C_3.\Psi$$

where

C_J : J^{th} column of M_{GV}

$\Psi^T = (\alpha_p, \beta_p, \gamma_p)$

The following expression represents the general $(i,j)^{th}$ term of the required transformation:

$$d_P \frac{dc_i}{\partial \mu_j} \cdot \Psi$$

μ_j = w, ϕ, K when j = 1, 2, or 3

The derivatives of the c_i vectors are determined from the basic rotation matrix description and are given as follows:

$$\frac{\partial c_1}{\partial w} = \begin{pmatrix} 0 \\ 0 \\ 0 \end{pmatrix}, \quad \frac{\partial c_1}{\partial \phi} = \begin{pmatrix} -m_{31} \text{ Cos K} \\ m_{31} \text{ Sin K} \\ \text{Cos } \phi \end{pmatrix}, \quad \frac{\partial c_1}{\partial K} = \begin{pmatrix} m_{21} \\ -m_{11} \\ 0 \end{pmatrix}$$

$$\frac{\partial c_2}{\partial w} = \begin{pmatrix} -m_{13} \\ -m_{23} \\ -m_{33} \end{pmatrix}, \quad \frac{\partial c_2}{\partial \phi} = \begin{pmatrix} -m_{32} \text{ Cos K} \\ m_{32} \text{ Sin K} \\ m_{31} \text{ Sin w} \end{pmatrix}, \quad \frac{\partial c_2}{\partial K} = \begin{pmatrix} m_{22} \\ -m_{12} \\ 0 \end{pmatrix}$$

$$\frac{\partial c_3}{\partial w} = \begin{pmatrix} m_{12} \\ m_{22} \\ m_{32} \end{pmatrix}, \quad \frac{\partial c_3}{\partial \phi} = \begin{pmatrix} -m_{33} \text{ Cos K} \\ m_{33} \text{ Sin K} \\ -m_{31} \text{Cos w} \end{pmatrix}, \quad \frac{\partial c_3}{\partial K} = \begin{pmatrix} m_{23} \\ -m_{13} \\ 0 \end{pmatrix}$$

From the discussion in appendix B concerning equation (A4),

$$\frac{\partial(w,\phi,K)}{\partial B} = E_N$$

and finally,

$$\frac{\partial(X_P,Y_P,Z_P)}{\partial B} = WE_N \qquad \text{(D2)}$$

where $w_{ij} = d_P \frac{\partial c_i}{\partial \mu_j} \cdot \Psi$

Let $\Delta P^T = (\Delta X_P, \Delta Y_P, \Delta Z_P)$, then

$$\Delta P = (Q_A, Q_B) \begin{pmatrix} \Delta A \\ \Delta B \end{pmatrix} \qquad \text{(D3)}$$

Q_A: 3 x 3(M+1) matrix of coefficients defined by equation (D1)

Q_B: 3 x 3(N+1) matrix of coefficients defined by equation (D2)

ΔA: 3(M+1) vector of model position errors

ΔB: 3(N+1) vector of model attitude errors

From equation (D3), the linear relation between exterior orientation errors and errors in the two computed ground points P_1 and P_2 is

$$\begin{pmatrix} \Delta P_1 \\ \Delta P_2 \end{pmatrix} = \begin{pmatrix} Q_{A_1} & Q_{B_1} \\ Q_{A_2} & Q_{B_2} \end{pmatrix} \begin{pmatrix} \Delta A \\ \Delta B \end{pmatrix}$$

and from equation (B7), the (6 x 6) covariance matrix for P_1 and P_2 is

$$\sigma_{P_1P_2} = \begin{pmatrix} Q_{A_1} & Q_{B_1} \\ Q_{A_2} & Q_{B_2} \end{pmatrix} \sigma_{EX} \begin{pmatrix} Q_{A_1}^T & Q_{A_2}^T \\ Q_{B_1}^T & Q_{B_2}^T \end{pmatrix} \qquad \text{(D4)}$$

Equation (D4) represents errors in P_1 and P_2 due solely to exterior orientation errors. Assume that the ground coordinate frame (G) pertains to a DTM, then the (4 x 4) covariance matrix $\sigma_{P_1' \; P_2'}$ represents the horizontal error of two points intersected in (G). The covariance matrix $\sigma_{P_1' \; P_2'}$ is obtained from $\sigma_{P_1 \; P_2}$ by deleting the 3rd and 6th rows and also by deleting the 3rd and 6th columns.

APPENDIX E. GRAY SHADE RELIEF IMAGE

A gray shade relief presentation is a mapping that converts regularly spaced elevation data into a terrain surface that is recognizable as such. The example derived in this Research Note used the Lommel-Seeliger model of a Lambertian surface to produce reflectance values for each elevation point.[1] A pseudoparallax is introduced so that a stereomate can be produced for stereo viewing.

Consider figure E1 where $\bar{S}$ is the direction to the fictitious sun, $\bar{V}$ is the direction to the viewer, and $\bar{N}p$ is normal to the slope at any point P in the terrain model:

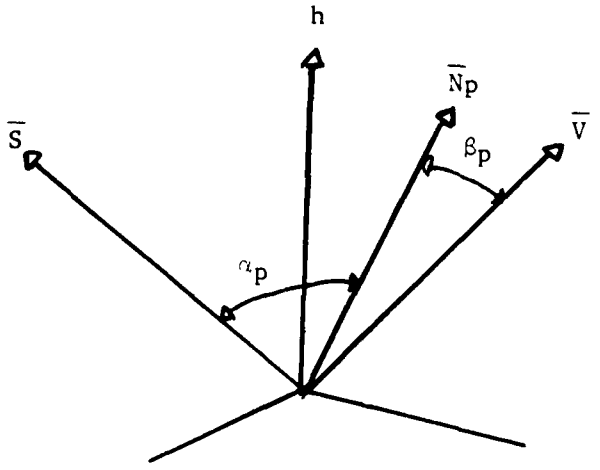

Figure E1. Reflectance Geometry.

[1] B. Horn, "Hill-Shading and the Reflectance Map," Proceedings: Image Understanding Workshop, Sponsored by: Information Processing Techniques Office, Defense Advanced Research Projects Agency, April 1979, pp. 79 to 120.

Directions to the fictitious sun and to the viewer are defined for convenience. For example, the azimuth and elevation to the sun in the horizontal plane can be selected to highlight a series of mountain ridges. The observer can be placed so that the resulting pseudoimage provides a useful perspective. In order to prevent line-of-sight ambiguities, $\bar{V}$, in the examples given in this Research Note, is perpendicular to the horizontal plane. The resulting pseudoimage is an orthographic representation of the terrain.

The Lommel-Seeliger reflectance model is defined as

$$R_p = \frac{1}{1 + \cos \beta_p / \cos d_p}$$

$$\cos \beta_p = \frac{\bar{N}p \cdot \bar{V}}{|\bar{N}p| \cdot |\bar{V}|}$$

$$\cos d_p = \frac{\bar{N}p \cdot \bar{S}}{|\bar{N}p| \cdot |\bar{S}|}$$

The slope vector $\bar{N}p$ is estimated from the digital terrain matrix. For example, if p refers to the $(i,j)^{th}$ location of the DTM, then

$$\bar{N}_p^T \simeq (-a, -b, 1)$$

$$a = (h_{i+1,j} - h_{i-1,j})/2\Delta Y$$

$$b = (h_{i,j+1} - h_{i,j-1})/2\Delta X$$

$(\Delta X, \Delta Y)$: horizontal spacing of X and Y in the DTM.

Valid reflectance values ($0 < R_p \leq 1$) are quantized to 256 gray shades for TV viewing.

Assume that a gray shade relief image of the terrain is constructed, one line at a time, according to the method given above. The stereomate is constructed by shifting each of its pixel locations along the line according to computed parallax values. Parallax is estimated by regarding

the two pseudoimages as vertical frame images. Consider the j^{th} point on the line, then if there is a change in elevation between the j^{th} and $(j+1)^{st}$ points, the parallax is

$$\Delta p \sim - (B/H) S_c (hj - hj+1)$$

$B/H > 0$: Base-Height

$S_c = D_c / D_G$: Scale

D_c : Length of TV line

D_G : 511δ

$\delta = \Delta X$: Horizontal ground spacing

Data is processed one line at a time. The objective is to compute a vector of coordinate values for the stereomate line that corresponds to a regularly spaced gray shade relief line of data. The computed coordinates will reflect the induced parallax. This operation will produce a set of irregularly spaced coordinates that correspond to the gray shades of the first line. Regularly spaced gray shades of the stereomate line are determined by interpolation.

Let $Q = S_c$ B/H, then the J^{th} coordinate of the first line is $X_{1j} = j - Q(h_{1j} - h_{11})$ where $X_{11} = 1$. If the first coordinate of the second line is shifted by $-Q(h_{21} - h_{11})$, then $X_{2j} = j - Q(H_{2j} - h_{11})$ and in general $X_{ij} = j - Q(h_{ij} - h_{11})$. Reflectance values pertaining to regularly spaced integer coordinates must be interpolated for in the irregularly spaced X-coordinates. The reflectance values used in the interpolation are those derived for the first image. Since, by construction, there is no y-parallax in the derived model, the two pseudoimages may be viewed quite readily in stereo, for example as an anaglyph.

APPENDIX F. ANAGLYPH REPRESENTATION

An anaglyph is a special form of a stereogram, which in turn is a three-dimensional image of the terrain derived from overlapping photographs using principles of stereoscopy. Consider the case where vertical and overlapping photographs are placed in a binocular device and in such a way that the observer can view the images concurrently, one with each eye. If the images are in the same plane and if the ocular base of the viewing device is parallel to the photographic base, then the images will fuse and produce a miniature model of the terrain. In the example described here, there is no y-parallax, which is to say corresponding lines of imagery are parallel to one another and to the ocular and photographic bases. This is exactly the situation between a gray shade relief image and its stereomate (see appendix E).

An anaglyph can be formed by projecting overlapping images in complementary colors onto a common plane. The anaglyph is viewed by an observer using glasses, where one lens is the first complementary color (such as red) and the second lens is the second complementary color (such as blue). A color TV display device can be used to construct anaglyphs from overlapping digital images or from a gray shade relief image and its stereomate. In the first case, the stereo pair may need to be reformatted to remove y-parallax. In either case, the images are displayed simultaneously and in complementary colors. The anaglyph is viewed by the observer using the appropriate glasses.

The measuring techniques used in analog operations can be applied in the digital realm. For example, consider the situation where overlapping images are viewed as an anaglyph. Digital image marks defining the line of sight for each eye can be superimposed on the anaglyph in complementary colors. If the marks are placed over corresponding image points, then the two will fuse and appear to lie on the image terrain. Since the location of the marks on the TV displays are uniquely related to the data base, the described operation is similar to the operation of a stereocomparator. In much of the digital image analysis at the Computer Sciences Laboratory, ETL, corresponding points are defined to be at regular line and sample intervals on the left image. Thus, if there is little or no y-parallax, the cursor on the right image can be moved along a TV line to affect correspondence. An application of these principles was tested and described more completely by ETL's Norvelle.[2]

---

[2]F. Norvelle, Interactive Digital Correlation Techniques for Automatic Compilation of Elevation Data, U.S. Army Engineer Topographic Laboratories, Fort Belvoir, VA, October 1981, ETL-0272, AD-A109 145.